Microstructural characterisation and microanalysis of creep resistant steels

M Wang[1], Y Chiu[1], I Jones[1], N Rowlands[2], J Holland[2], Z Zhang[3] and D Flahaut[4]
[1]School of Metallurgy and Materials, University of Birmingham, Birmingham, B15 2TT, UK
[2]Oxford Instruments NanoAnalysis, Halifax Road, High Wycombe, HP12 3SE, UK
[3]Doncasters Technical Centre, George Baylis Road, Worcestershire, WR9 9RB, UK
[4]Doncasters Paralloy Ltd, Paralloy House, Nuffield Road, Cleveland, TS23 4DA, UK
E-mail: MXW158@bham.ac.uk

Abstract: Steels for high temperature applications require good creep resistance which is controlled by the chemistry and microstructure of the materials. This paper focuses on the microstructural characterisation of a creep resistant steel using electron microscopy. The existence of various primary carbides, e.g. NbC, M_7C_3 and $M_{23}C_6$ was confirmed by electron diffraction. The primary chromium carbides transformed from M_7C_3 to $M_{23}C_6$ during creep while the niobium carbides were nearly unaltered. In addition, secondary precipitates ($M_{23}C_6$) were observed within the matrix after creep. The size and distribution of the secondary carbides were analysed by a 80 mm^2 windowless X-Max^N SDD at 3 kV on an SEM. Scanning transmission electron microscopy (STEM) observations showed the appearance of fine NbC, G phase ($Ni_{16}Nb_6Si_7$) and (Nb, Ti)(C, N) particles.

1. Introduction

As the service conditions in steam reforming involve a high temperature and a high pressure, the materials for this application require superior creep resistance [1]. One of the basic ways in which creep resistant steels can be strengthened is by precipitation. The precipitates, such as M_7C_3, $M_{23}C_6$ and MX, play an important role in the achievement of good creep properties. Traditional Si(Li) detectors, however, have a relatively poor performance in the identifications of carbides or nitrides due to limited spatial resolution. Silicon drift detectors (SDD), which were invented by Gatti and Rehak in 1984 [2], have become very powerful instrumentation tools for industrial and scientific application in X-ray spectroscopy due to their good energy resolution, high count rate capability and convenient experimental conditions [3]. Furthermore, a new generation of windowless SDD enhances the collection efficiency for low energy X-rays to improve any analyses which need to be based on low energy lines, such as Nb M lines. The present work focuses on microstructure characterisation and microanalysis of creep resistant steels by using windowless SDD on both SEM and TEM.

2. Experimental Methods

A creep resistant steel --- *Alloy A* was supplied by Doncasters Group Ltd. The alloy was crept at 1000˚C and 40 MPa for 12 hours. Back-scattered electron (BSE) imaging and energy dispersive X-ray spectrometry (EDS) were used to investigate the element distribution. The size and distribution of the

secondary chromium carbides were analysed with an 80 mm^2 windowless X-Max^N SDD at 3 kV on an FEG-SEM. Scanning transmission electron microscopy (STEM) was carried out on a Tecnai F20 TEM operating at 200 kV with an 80 mm^2 windowless X-Max^N TLE SDD.

3. Results and discussion

3.1 As-cast microstructure

Figure 1 (a) shows the microstructure of as-cast *Alloy A*. The grains are surrounded by Nb-rich carbides and Cr-rich carbides which form a fragmented network. Nb is confined to the primary carbide network [4], whereas Si and Fe remain in solid solution in the Ni-rich matrix. The EDS analyses show that the concentration of carbon in the chromium carbide is around 30 at.%, which indicates that it should be the M_7C_3 type. As shown in Table 1, Ni and Fe are found to substitute partially for Cr [5]. No fine precipitation has been observed in the matrix.

Table 1 EDS analyses obtained from the points shown in Figure 1

Atomic %	C	Si	Cr	Fe	Ni	Nb
1—Cr-carbides (as-cast)	31.85±0.72	---	59.63±1.13	7.30±0.68	1.21±0.22	---
2—Nb-carbides	41.73±0.81	---	9.56±1.33	3.46±0.52	2.67±0.14	42.36±0.33
3—Matrix	6.99±0.67	2.12±0.54	22.41±1.04	35.77±0.43	31.94±0.20	---
4—Cr-carbides (crept)	21.67±1.21	---	66.26±0.84	8.35±0.39	3.02±0.47	---

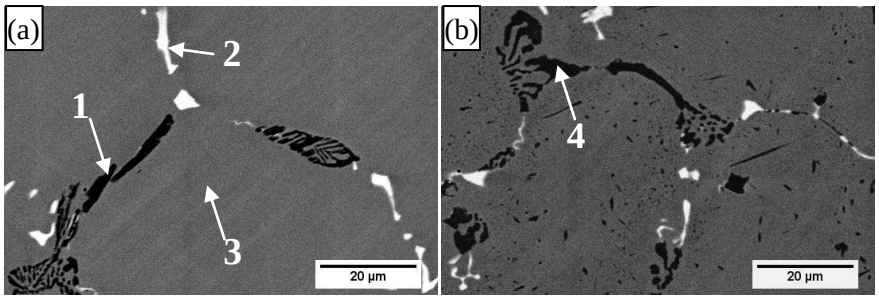

Figure 1 BSE micrograph obtained from (a) as-cast *Alloy A* and (b) crept *Alloy A*

3.2 Microstructure evolution

The microstructure of the crept *Alloy A* is illustrated in Figure 1 (b). The content of carbon in primary chromium carbides decreased from 30% to 21% (c.f. Table 1), indicating transformation from M_7C_3 to $M_{23}C_6$. The NbC morphologies are nearly unaltered during the creep, except for slight coarsening. Secondary precipitation can be observed within the matrix resulting from the supersaturated solid solution of carbon. Figures 2 (a-d) shows the results, using an SEM operating at 3 kV, of background and overlap corrected X-ray mapping (AZtec TruMap). The X-ray lines used in the SEM were low energy Cr L and Nb M, while the lines used in the TEM were Cr K and Nb K. Although the spatial resolution is not as good as that using TEM (c.f. Figures 2 (e-h)), they are in agreement that secondary chromium carbides are 100~250 nm. The secondary chromium carbides of such a size can act as barriers to dislocation movement contributing to good creep resistance.

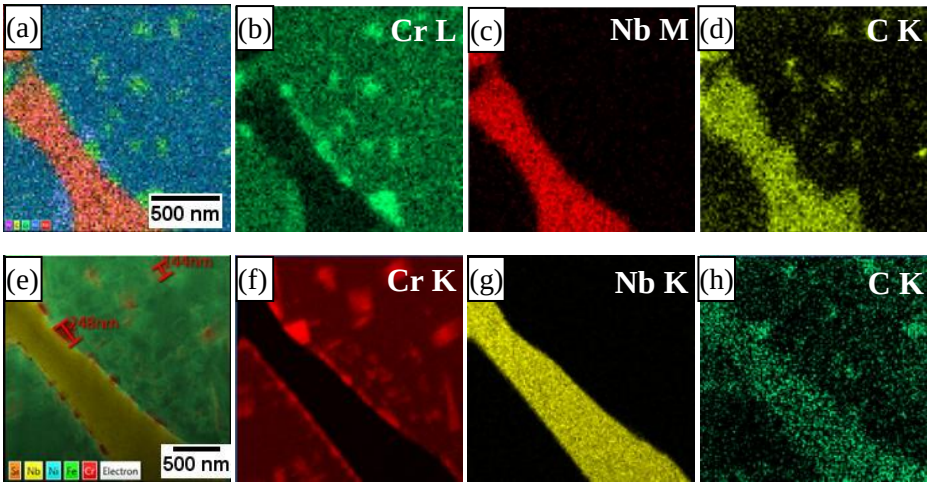

Figure 2 Overlap corrected TruMaps collected on (a-d) SEM at 3kV with an 80 mm^2 windowless X-Max^N SDD (e-h) TEM at 200 kV with an 80 mm^2 windowless X-Max^N TLE SDD

3.3 TEM observations

As shown in Figure 3, the STEM analysis was carried on a selected area of crept *Alloy A* containing a primary chromium carbide. Nb carbides were mainly observed at the interface between the primary chromium carbide and the matrix. A Nb-Ni-Si particle was found associated with the primary chromium carbide; it has a fcc structure with a lattice parameter of 1.13 nm identifying it as G-phase ($Ni_{16}Nb_6Si_7$). Although G phase does not appear to be intrinsically detrimental to the mechanical properties, the transformation from NbC (a=0.44 nm) into G phase (a=1.12 nm) induces a volume expansion and leads to cracking along the grain boundary.

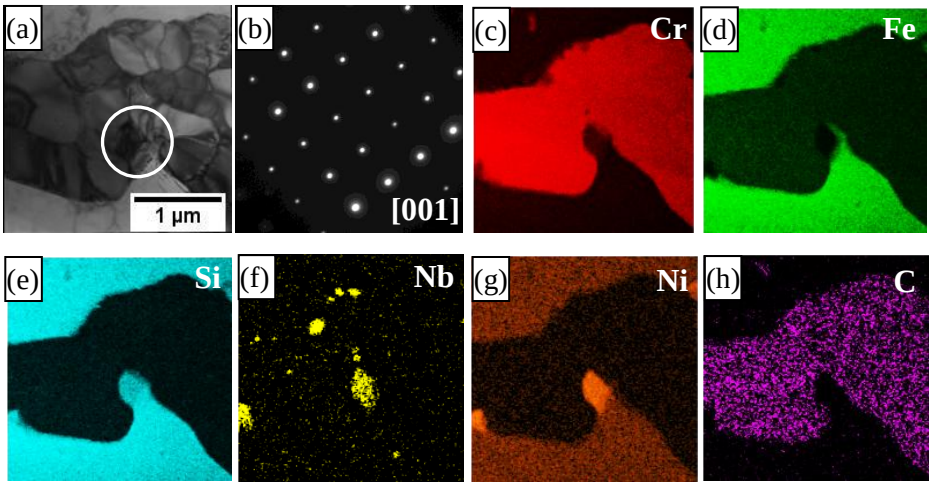

Figure 3 Cr carbide (a) bright field image; (b) selected area diffraction and (c-h) overlap corrected TruMaps

The EDS spectrum shows that the fine particle highlighted in Figure 4 (a) is rich in chromium, niobium, carbon and nitrogen. However, the contents of Nb, Cr and N are different from that of a typical nitride such as Z-phase (NbCrN) in austenitic stainless steel [6]. The diffraction patterns

obtained from the particle were indexed as fcc with a lattice parameter of 0.429 nm close to NbC with its lattice parameter of 0.44 nm. EDS mapping shown in Figure 5 leads to a similar result --- observation of a (Nb, Ti)(C, N) particle combined with a chromium carbide.

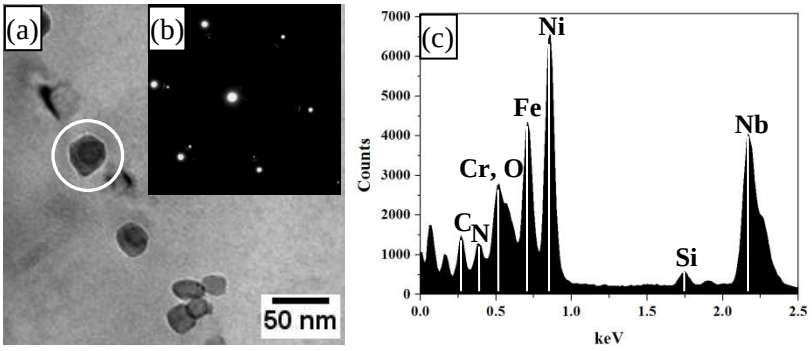

Figure 4 Selected particles (a) bright field image; (b) selected area diffraction and (c) EDS spectrum

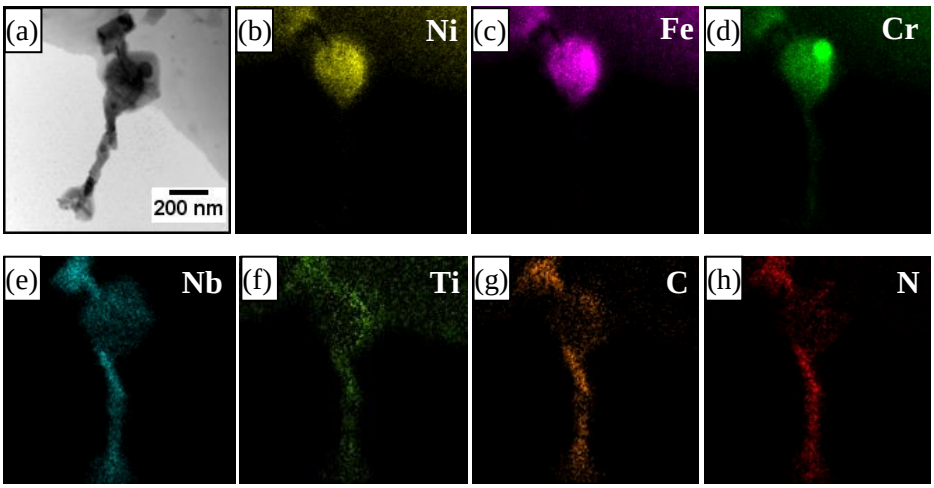

Figure 5 (Nb, Ti)(C, N) particle (a) bright field image and (b-h) overlap corrected TruMaps

4. Conclusion

- The existence of NbC, M_7C_3 and $M_{23}C_6$ was confirmed;
- The primary chromium carbides transformed from M_7C_3 to $M_{23}C_6$ during creep;
- Secondary chromium carbides $M_{23}C_6$ (100~250 nm) were observed within the matrix;
- Scanning transmission electron microscopy (STEM) showed the appearance of fine NbC, G phase ($Ni_{16}Nb_6Si_7$) and (Nb, Ti)(C, N) particles.

Reference

[1] Yan J B *et al Mat Sci Eng A-Struct.* **529** (2011) 361-369.
[2] Gatti E *et al Nucl Instrum Meth A.* **226** (1984) 129-141.
[3] Gatti E and Rehak P *Nucl Instrum Meth A.* **541** (2005) 47-60.
[4] Wang W Z *et al Mater Design.* **32** (2011) 4010-4016.
[5] Sourmail T *Mater Sci Tech Ser.* **17** (2001) 1-14.
[6] Danielsen H K and Hald J *Mat Sci Eng A-Struct.* **505** (2009) 169-177.